Special issue of the 3rd International Conference on Computational and Experimental Science and Engineering (ICCESEN 2016)

Synthesis, Characterization and Cr(VI) Adsorption Properties of Modified Magnetite Nanoparticles

H. Çiftçi[a,*], B. Ersoy[a] and A. Evcin[b]

[a]Afyon Kocatepe University, Mining Engineering Department, Afyonkarahisar, Turkey

[b]Afyon Kocatepe University, Material Science and Engineering Department, Afyonkarahisar, Turkey

In this study, magnetite (Fe_3O_4) nanoparticles were synthesized by chemical co-precipitation method, coated with silica, and then the surface of silica coated magnetite (Fe_3O_4@SiO_2) nanoparticles was modified with (3-aminopropyl)triethoxysilane (APTES) at first. Secondly, attained nanoparticles were characterized by the Fourier transform infrared, X-ray diffraction, transmission electron microscopy, the Brunauer–Emmett–Teller, vibrating sample magnetometer, and zeta-sizer devices/methods. Finally, detailed adsorption experiments were performed to remove hexavalent chromium (Cr(VI)) from aqueous media by synthesized nanoparticles. Mean size and specific surface area of synthesized nanoparticles were about 15 nm and 89.5 m^2/g, respectively. The highest adsorption capacity among used adsorbents (Fe_3O_4, Fe_3O_4@SiO_2, Fe_3O_4@SiO_2@L) was attained by Fe_3O_4 nanoparticles and it was determined that adsorption capacity of the other two adsorbents was too low when compared to the Fe_3O_4 nanoparticles. Optimum conditions for Cr(VI) adsorption by Fe_3O_4 nanoparticles were: pH, 3; temperature, 55 °C; contact time, 90 min; adsorbent concentration, 0.5 g/l and initial Cr(VI) concentration 10 mg/l. Under these conditions, adsorption capacity and removal percentage of Cr(VI) were found to be 33.45 mg/g and 88%, respectively.

DOI: 10.12693/APhysPolA.132.564

PACS/topics: nanomagnetite, adsorption, Cr(VI), Langmuir, Freundlich, adsorption kinetics

1. Introduction

Nanoparticles (NPs) are of great interest in recent years due to their outstanding chemical, physical, and magnetic properties which are different from coarse-grained counterparts [1–4]. Magnetite nanoparticles (Fe_3O_4 NPs) have also attracted a great attention to use as a new adsorbent, in analytical chemistry and for medicine researches with their some advantageous properties such as high surface area, low cost, high magnetic sensitivity, and high surface-active area [5]. Furthermore, Fe_3O_4 NPs are also used for some specific applications, such as drug delivery, magnetic field-assisted cancer therapy, cell labelling and sorting, magnetic resonance imaging and sensing. Like this there are various applications of Fe_3O_4 NPs, but they are not very stable under different environmental conditions, can turn into maghemite by oxidation and soluble in strongly acidic media [6–9]. In order to overcome these problems, the surface of Fe_3O_4 NPs can be layered with a protective material. Silica is the best known material to coat the surface of Fe_3O_4. Silica has a good mechanical and chemical stability and so silica coating provides Fe_3O_4 NPs to stay stable and prevents to dissolve in acidic media [10]. Furthermore, silica is biocompatible and there are plenty of silane groups on the silica surface. Therefore, silica coated magnetite (Fe_3O_4@SiO_2) NPs can easily be modified by various functional groups [11]. The surface of Fe_3O_4@SiO_2 NPs is negatively charged in aqueous media at low pH levels. In this case, the adsorption of anionic ions on the negatively charged surface would be difficult because of electrostatic repulsion forces. The surface of silica can also be modified by various techniques and chemicals (especially by amine groups) to obtain positively charged surface. In this study, (3-aminopropyl)triethoxysilane was used to modify the surface of Fe_3O_4@SiO_2 NPs.

Chromium is one of the most important toxic and heavy metals emitted into the environment and used in various applications such as leather industry, catalyst manufacturing, paint and ink industries, ceramic and glass industry, photography, chromium-plating and production of chromium alloys or metals [12, 13]. Hexavalent chromium ($HCrO_4^-$, CrO_4^{2-}, $Cr_2O_7^{2-}$) and trivalent chromium (Cr^{3+}, $Cr(OH)^{2+}$) are two main chromium forms mostly occurring in the aquatic environment as a result of various processes [14]. Unlike other chromium components, hexavalent chromium [Cr(VI)] is soluble in groundwater and therefore its transportation and participation to living organisms is much more likely. Most of the components of Cr(VI) has been reported to be toxic, carcinogenic and mutagenic [15, 16]. According to the World Health Organization (WHO) standards, maximum allowable Cr(VI) concentration in drinking waters is 0.05 mg/l [13, 17]. Thus, the amount of chromium content in the waste waters which have dangerous effect on living beings should be reduced to minimum level before releasing into the environment.

In this study, adsorption technique which is more economic, efficient, and easier technique than other techniques was used to remove Cr(VI) ions from aqueous media by magnetite and modified magnetite NPs. There is a key role of the surface properties of magnetite for Cr(VI) adsorption. In acidic media, magnetite surface becomes more positive and so anionic Cr(VI) ions can

*corresponding author; e-mail: hciftci@aku.edu.tr

easily be adsorbed on the magnetite surface by the effect of electrostatic attraction forces [18]. In addition, the magnetic sensitivity of magnetite also affects the removal of Cr(VI) [19].

2. Materials and methods

2.1. Materials

Ammonium hydroxide (NH_4OH, 28.0–30.0%) and 1,5-diphenylcarbazide ($C_{13}H_{14}N_4O$) were purchased from Sigma Aldrich. (3-aminopropyl)triethoxysilane ($C_9H_{23}NO_3Si$, 98%) was purchased from Alfa. Iron(II) chloride hexahydrate ($FeCl_3{\cdot}6H_2O$, > 98%), iron(III) chloride tetrahydrate ($FeCl_2{\cdot}4H_2O$, > 99%), tetraethylorthosilicate ($Si(OC_2H_5)_4$, 28%), hydrochloric acid (HCl, 35–37% GR), sodium hydroxide (NaOH, 96%), sulphuric acid (H_2SO_4, 95–97%), potassium dichromate ($K_2Cr_2O_7$), acetone (C_3H_6O) and ethanol (C_2H_5OH, 99.7%) were purchased from Merck.

Cr(VI) stock solution (500 mg/l) was prepared by dissolving 1.414 g $K_2Cr_2O_7$ with 1000 ml distilled water. 1.5-DPC (0.5%) solution was used for UV measurements and prepared by dissolving 0.25 g 1.5-diphenylcarbazide with 50 ml acetone. 6N sulphuric acid solution was prepared by adding 8.33 ml H_2SO_4 (98%) into 50 ml distilled water to be used to pH adjustments at UV measurements.

2.2. Synthesis of nanoparticles

In this study, modified Massart technique was used to synthesize magnetite NPs [20]. Briefly, 0.02 mol $FeCl_3{\cdot}6H_2O$ and 0.01 mol $FeCl_2{\cdot}4H_2O$ were dissolved with 100 ml distilled water in a five-necked flask at room temperature. Dissolution and stirring was carried out for 30 min at 750 rpm using a mechanical stirrer. Then 50 ml of 28% concentrated NH_4OH was added dropwise (3.3 ml/min) into the solution. After that the solution temperature was increased to 90 °C and stirring was continued for 2 h. Finally, the obtained magnetite NPs precipitate was separated from solution using a magnet, washed distilled water and ethanol several times and stored at 1% concentration in ethanol. Fe_3O_4@SiO_2 NPs were prepared according to the Stöber method by applying some changes [10, 21]. 50 ml of previously prepared magnetite liquid (1%) was dispersed ultrasonically and then added into a 500 ml three-necked flask which contained 40 ml distilled water, 120 ml ethanol, and 5 ml NH_4OH (28%). The mixture was stirred for 30 min at 25 °C and 800 rpm using a mechanical stirrer and after stirring 0.4 ml TEOS was added into the mixture very slowly (0.013 ml/min). After adding TEOS, stirring was continued for another 4 h under the same conditions. Finally, the silica coated magnetite NPs were taken from solution by a magnet, washed distilled water and ethanol several times and stored at 1% concentration in ethanol. In order to prepare amine modified NPs (Fe_3O_4@SiO_2@L), the following method was summarized. 150 mg Fe_3O_4@SiO_2 powder was put in a 100 ml beaker which contained 50 ml ethanol and the mixture dispersed ultrasonically at 80 W for 2 min. After that 1 ml APTES was added into the mixture and stirred for 3 h at 50 °C. After stirring, modified NPs were separated from solution and dried for 4 h at 65 °C. All synthesis processes were performed under N_2 gas to prevent oxidation of NPs. A schematic summary of the synthesis steps is given in Fig. 1.

Fig. 1. Schematic illustration of summarized synthesis process of NPs.

2.3. Characterization methods

The morphology and size of NPs were observed using JEM 2100F (JEOL) transmission electron microscope (TEM). To determine the functional groups of NPs, the Fourier transform infrared (FTIR) spectra were recorded on a Perkin–Elmer Spectrum BX spectrometer with the KBr technique in the range of 400–4000 cm^{-1}. Magnetic sensitivities were determined by using 1.2 H vibrating sample magnetometer VSM (LDJ 9600) at 200 kV accelerated voltage. To understand the crystal structure of NPs, Bruker D8 advance X-ray diffraction device (XRD) was used with Cu K_α radiation. The specific surface area of NPs was determined using Micromeritics Gemini 2360 by the Brunauer, Emmett and Teller (BET) method [22]. Zeta potential (ζ) measurements were performed using Malvern Nano-Z zetasizer. To perform ζ measurements 0.01 g of sample with 100 ml 10^{-3} M NaCl solution were put in a beaker and the mixture was dispersed ultrasonically for 3 min. Then, pH of mixture was adjusted using previously prepared 0.1–5 M HCl and 0.1–1 M NaOH solutions and ζ measurements were performed for each sample.

2.4. Adsorption experiments

Batch adsorption experiments were performed in a 100 ml erlenmayer which contained 50 ml Cr(VI) solution of known concentration and desired amount of adsorbent. The mixture was stirred using a GFL-1086 shaking water bath at 175 rpm. After that the adsorbent was taken from solution by magnetic separation using a magnet and the solution analysed for the residual Cr(VI) ions by Shimadzu UV-1240 spectrophotometer. Determination of Cr(VI) ions was performed as follows. 40 ml of sample was taken in a beaker and 3 ml of 6N H_2SO_4 was added into the solution to decrease the pH of the solution under 2. Then 0.8 ml of 0.5% DPC solution was added to the mixture. After waiting for 5 min, the UV measurements were performed [23]. Percentage removal of Cr(VI) and amount of adsorption at equilibrium, q_e (mg/g), were calculated by using following Eqs. (1) and (2):

$$\text{Removal}(\%) = \frac{C_i - C_e}{C_i} \times 100\%, \tag{1}$$

$$q_e = \frac{C_i - C_e}{m} \times V, \quad (2)$$

where C_i and C_e are the initial and final concentration of Cr(VI) ions (mg/l) in the solution, respectively. V is the volume (l) of tested solution and m is the mass of used adsorbent (g).

3. Results and discussion

3.1. Characterization of synthesized nanoparticles

FTIR spectrum of synthesized NPs is displayed in Fig. 2. Strong adsorption band around 570–580 cm^{-1} wavelength proves the presence of Fe_3O_4 NPs for both spectra. This band is interpreted to stretching vibrations of Fe^{2+} and Fe^{3+} ions in tetrahedral regions and Fe^{3+} ions in octahedral regions of magnetite [8]. The absorption bands at 945 cm^{-1} and 1094 cm^{-1} wavelength observed in Fig. 2b are a result of Si–O–Si and Si–O–H stretching vibrations. The extra peak seen at 800 cm^{-1} wavelength is due to the Si–O vibration [24]. These results indicate that the magnetite NPs was successfully coated by silica. The wide bands around 3440 cm^{-1} wavelength are attributed to O–H stretching vibrations of free water molecules, hydroxyl groups (OH) on the surface, or water molecules absorbed by the material [8, 9].

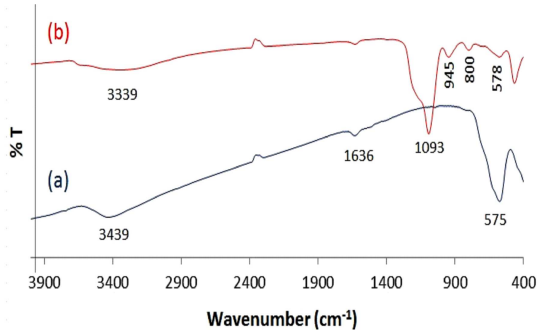

Fig. 2. FTIR spectra of Fe_3O_4 NPs (a) and Fe_3O_4@SiO_2NPs (b).

TEM images of the NPs were shown in Fig. 3. The average particle size of Fe_3O_4 NPs was estimated to be 15 nm and silica shell thickness was not clearly seen because of very thin coating. Therefore, surface coating and modification have no significant effect in size and morphology of Fe_3O_4 NPs. The NPs has approximately spherical shape as seen in the figure.

Figure 4 shows the XRD pattern of NPs. Large peaks show nanocrystalline and sharp peaks show the high degree of crystalline structure [8, 25]. As seen in the figure, crystalline diffraction peaks with 2θ at 30.1°, 35.4°, 43.2°, 53.9°, 57.2° and 62.7° correspond to the characteristic planes [(220), (311), (400), (422), (511), (440)] of cubic spinel Fe_3O_4, respectively (JCPDS No. 01-071-6336). The same results observed in Fig. 4b indicate the presence of magnetite crystals. As shown in XRD pattern of Fe_3O_4@SiO_2@L NPs, less intense and larger peaks are a result of silica coating and amine modification of the magnetite surface [26].

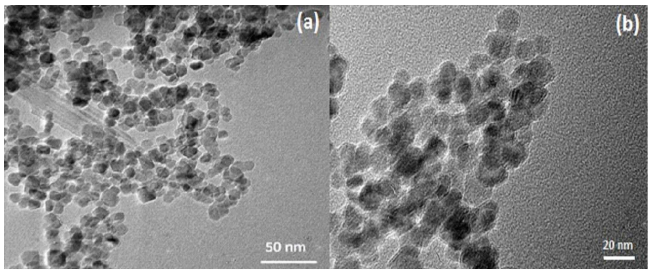

Fig. 3. TEM micrographs of Fe_3O_4 NPs (a) and Fe_3O_4@SiO_2@L NPs (b).

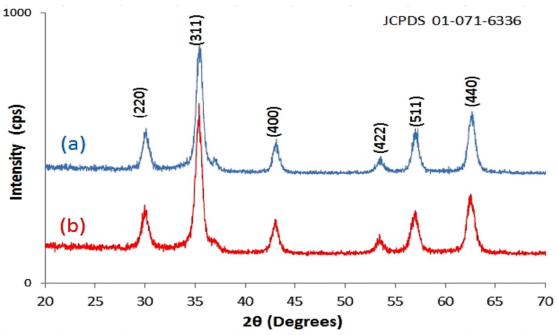

Fig. 4. XRD patterns of Fe_3O_4 NPs (a) and Fe_3O_4@SiO_2@L NPs (b).

Magnetization curves of synthesized NPs are given in Fig. 5. Magnetization saturations (M_s) of Fe_3O_4 and Fe_3O_4@SiO_2@L NPs were found to be 75 emu/g and 37 emu/g, respectively. As expected, the magnetization saturation of Fe_3O_4@SiO_2@L NPs measured was lower and this is a result of diamagnetic silica shell mass surrounding the magnetite NPs. But, 37 emu/g is still sufficient for magnetic separation of NPs by a magnet from a solution. Another result shown in Fig. 5 is that both magnetization curves go through exactly the origin of magnetization graph. This means that the synthesized NPs show superparamagnetic behaviour at room temperature because of not exhibiting hysteresis, coercivity, and remanence [27].

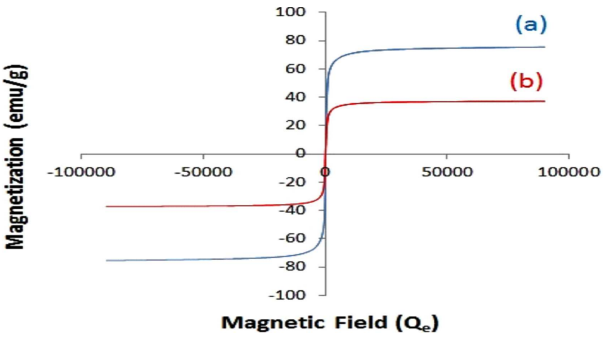

Fig. 5. Magnetization curves of (a) Fe_3O_4 and (b) Fe_3O_4@SiO_2@L NPs.

In order to determine the surface charge of NPs, ζ measurements as a function of pH are presented in Fig. 6. As seen in the figure, the isoelectric point (iep) of Fe_3O_4

NPs was found to be 6.8 which is compatible with literature values [8, 27, 28]. The Fe_3O_4@SiO_2NPs showed an iep of 2.2 close to that of amorphous silica [29] and the iep of Fe_3O_4@SiO_2@L NPs was measured to be 8.4. These different results prove that silica coating and amine modification of magnetite NPs surface were successfully performed.

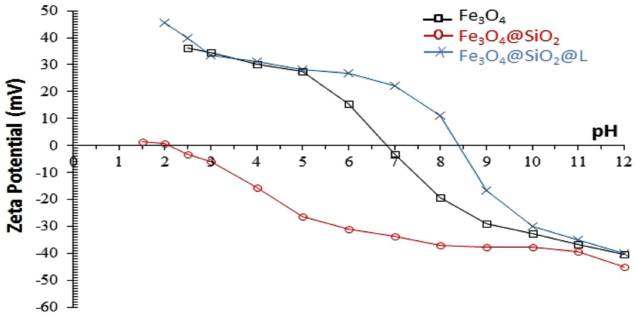

Fig. 6. Zeta potential (ζ) measurements of NPs as a function of pH.

3.2. Comparison of prepared NPs according to their adsorption capacities

Adsorption experiments at different initial Cr(VI) concentrations were performed to compare the adsorption capacities of NPs and obtained comparative results are shown in Fig. 7. When adsorption experiments were performed, the temperature was 25 °C, contact time: 90 min, adsorbent concentration: 0.5 g/l, and pH was kept at 2. As clearly shown in the figure, adsorption capacity of Fe_3O_4@SiO_2 and Fe_3O_4@SiO_2@L NPs (1.0 mg/g and 3.2 mg/g, respectively) was found to be much lower than Fe_3O_4NPs (25 mg/g). Therefore, Fe_3O_4 adsorbent was selected to perform the next detailed adsorption experiments.

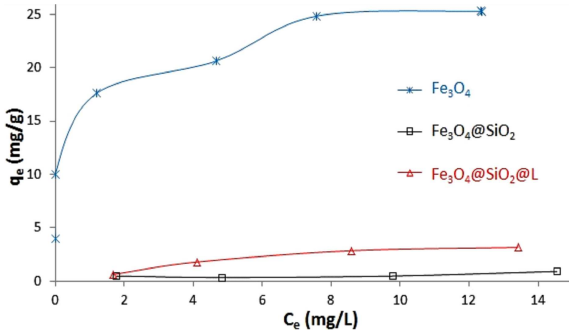

Fig. 7. Cr(VI) adsorption capacities of prepared NPs (adsorption conditions: initial concentration of Cr(VI) 10 mg/l, adsorbent dose 0.5 g/l, contact time 24 h, temperature 25 °C).

3.3. Effect of pH

Figure 8 shows the effect of pH on the adsorption of Cr(VI) ions by Fe_3O_4 NPs. Maximum removal percentage of Cr(VI) (88%) was found at pH range 2–3. As clearly seen in the figure, the increase of pH resulted in a sharp decrease of Cr(VI) removal. The dominant form of Cr(VI) at 2–20 mg/l concentrations and acidic pH levels is $HCrO_4$ which occurs from the hydrolysis reaction of the $Cr_2O_7^{2-}$ ions. If pH value becomes greater than 6.5, CrO_4^{2-} ions are seen as dominant Cr(VI) form [30]. Electrostatic attractive forces between the positively surface charged adsorbent and anionic adsorbate ($HCrO^{-4}$) are the main cause of the high adsorption amount at acidic pH levels. pH 3 was selected as optimum value for the further experiments. The iep of adsorbent (Fe_3O_4) was found to be 5.8. Therefore, the surface of adsorbent is negatively charged at pH higher than 5.8 and so adsorption of Cr(VI) becomes difficult due to electrostatic repulsion forces.

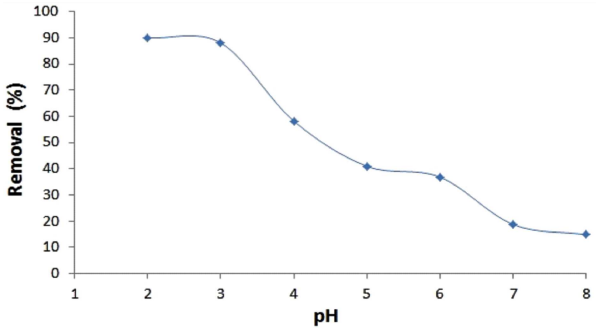

Fig. 8. Effect of pH on the removal of Cr(VI) by Fe_3O_4 NPs (adsorption conditions: initial concentration of Cr(VI) 10 mg/l, adsorbent dose 0.5 g/l, contact time 24 h, temperature 25 °C).

3.4. Effect of adsorbent dose

The effect of adsorbent dose on removal of Cr(VI) ions from solution is demonstrated in Fig. 9. Experimental results showed that the percentage removal of Cr(VI) increased from 42.5% to 100% with increasing amount of adsorbent dose from 0.2 g/l to 0.8 g/l. This can be explained with increase of effective surface area on which metal ions will be adsorbed. On the other hand, the adsorption capacity (mg/g) was continuously decreased with increase of adsorbent dose and this situation is a result of remaining of effective surface area without saturation along with the adsorption process. Similar results were also observed in the other experiments using different adsorbents to removal of Cr(VI) [15, 31]. When viewed economically, 0.5 g/l was selected as optimum adsorbent dose for the next experiments.

3.5. Effect of initial Cr(VI) concentration and contact time

Figure 10 shows the change in adsorption capacity with the change of initial Cr(VI) concentration from 5 to 25 mg/l and contact time up to 150 min. As it is expected, a rapid increase in the adsorption capacity was observed in the first stage and then this increase was slowed down until adsorption process reached the equilibrium time. Adsorption capacity increased from 17.4 mg/g to 24.9 mg/g when percentage removal decreased from 87.5% to 62.2% by increase of the initial

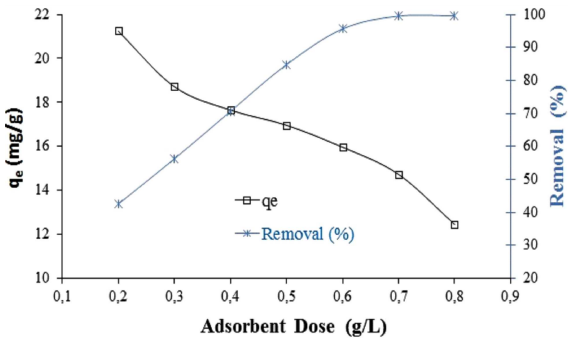

Fig. 9. Effect of adsorbent dose on the removal of Cr(VI) by Fe_3O_4 NPs (adsorption conditions: initial concentration of Cr(VI) 10 mg/l, contact time 90 min, temperature 25 °C, pH 3).

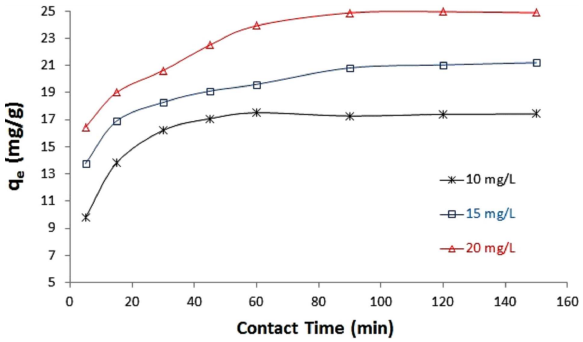

Fig. 10. Effect of contact time and initial Cr(VI) concentration on the removal of Cr(VI) by Fe_3O_4 NPs (adsorption conditions: amount of adsorbent 0.5 g/l, temperature 25 °C, pH 3).

Cr(VI) concentration from 10 mg/l to 20 mg/l. This situation can be explained by the mass transfer rate resulted from growing driving force [32]. Additionally, the curves reaches an equilibrium at 90 min and initial Cr(VI) concentration has no effect on the equilibrium time. According to these results, it can be said that the adsorption of Cr(VI) on the surface of Fe_3O_4 NPs is monolayer [33].

3.6. Effect of temperature

Effect of temperature on Cr(VI) removal as a function of initial chromium concentration is illustrated in Fig. 11. As seen clearly from figure, the adsorption capacity (mg/g) increased with increase of temperature and this result indicates that the adsorption of Cr(VI) on Fe_3O_4 NPs is a endothermic process. When the adsorption process reached equilibrium, maximum adsorption capacities at 25 and 55 degrees was found to be 25 mg/g and 35 mg/g, respectively.

3.7. Adsorption mechanism

In this study, the target ions were the $HCrO_4$ ions which are the dominant form of Cr(VI) ions at 10–25 mg/l initial concentration range and pH 3. In aqueous media, $FeOH_2^+$ functional groups are formed on the surface of Fe_3O_4 NPs [34]. Adsorption of $HCrO_4$ ions on the Fe_3O_4 NPs is a physicochemical process according to other studies. Namely, Cr(VI) ions are adsorbed

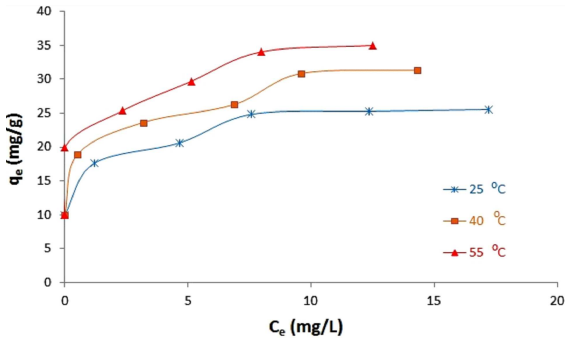

Fig. 11. Effect of temperature on the removal of Cr(VI) by Fe_3O_4 NPs (adsorption conditions: initial concentration of Cr(VI) 10 mg/l, contact time 90 min, adsorbent concentration 0.5 g/l, pH 3).

physically on the surface of Fe_3O_4 NPs by electrostatic attraction forces and then reduced to Cr(III) by redox reactions [35–37]. After physical adsorption process, chemical adsorption happens by electron exchange between $FeOH_2^+$ and $HCrO_4$ ions, and Cr(VI) ions are reduced to non-toxic Cr(III) forms. Another way to understand this physical or chemical mechanism of the adsorption is calculation of adsorption energy. If adsorption energy becomes in the range of 1–2 kJ/mol, physical adsorption process is observed. 20–40 kJ/mol adsorption energy levels show the chemical adsorption process [38]. According to thermodynamic calculations in this study the adsorption energy (E_a or ΔH^o) was found to be 23.45 kJ/mol. Therefore, we can say that the adsorption of Cr(VI) ions onto the Fe_3O_4 NPs is a chemical process.

4. Conclusion

Fe_3O_4 NPs have been shown to be an effective adsorbent for adsorption of Cr(VI) when compared to Fe_3O_4@SiO_2 and Fe_3O_4@SiO_2@L NPs. Electrostatic attraction forces between Cr(VI) ions and magnetite NPs play a key role for the Cr(VI) removal. The adsorption process was found to be strongly dependent on pH, contact time, adsorbent dose, and initial Cr(VI) concentration. Maximum Cr(VI) adsorption capacity was found to be 33.45 mg/g with 88% removal at pH 3.0. According to these results, Fe_3O_4 NPs can be used as an effective adsorbent for removal of Cr(VI) ions from industrial waste waters. Additionally, the magnetic separation of Fe_3O_4 NPs from solution is more rapid, simpler, and more effective than other solid–liquid separation techniques.

Acknowledgments

This study was financially supported by Afyon Kocatepe University, Scientific Research Projects (BAP), Project No. 14.FEN.BIL.33.

References

[1] W. Laslouni, Z. Hamlati, M. Azzaz, *Acta Phys. Pol. A* **128**, B-190 (2015).

[2] W. Laslouni, M. Azzaz, *Acta Phys. Pol. A* **130**, 112 (2016).

[3] H. Mutuk, T. Mutuk, H. Gümüs, B. Mesci Oktay, *Acta Phys. Pol. A* **130**, 172 (2016).

[4] F. Göde, F. Yavuz, I.A. Kariper, *Acta Phys. Pol. A* **128**, B-215 (2015).

[5] A.F. Ngomsik, A. Bee, M. Draye, G. Cote, V. Cabuil, *Compt. Rend. Chim.* **8**, 963 (2005).

[6] H. Bagheri, A. Afkhami, M. Saber-Tehrani, H. Khoshsafar, *Talanta* **97**, 87 (2012).

[7] F. Fajaroh, H. Setyawan, A. Nur, W. Lenggoro, *Adv. Powd. Technol.* **24**, 507 (2013).

[8] M.H. Farimani, N. Shahtahmasebi, M. Rezaee Roknabadi, N. Ghows, A. Kazemi, *Physica E* **53**, 207 (2013).

[9] Y.S. Li, J.S. Church, A.L. Woodhead, F. Moussa, *Spectrochim. Acta A* **76**, 484 (2010).

[10] Y.H. Deng, C.C. Wang, J.H. Hu, W.L. Yang, S.K. Fu, *Coll. Surf. A Physicochem. Eng. Asp.* **262**, 87 (2005).

[11] Y. Xu, Y. Zhou, W. Ma, *J. Nanopart. Res.* **15**, 1716 (2013).

[12] W. Slooff, *Integrated Criteria Document Chromium*, Report no. 758701002, National Institute of Public Health and Environmental Protection, Bilthoven, Netherlands 1989.

[13] World Health Organization (WHO), *Chromium, Environmental Health Criteria*, No. 61, Geneva 1988.

[14] U. Förstner, G.T.W. Wittmann, *Metal Pollution in the Aquatic Environment*, 2nd ed., Springer-Verlag, Berlin 1981.

[15] H. Li, Z. Li, T. Liu, X. Xiao, Z. Peng, L. Deng, *Biores. Technol.* **99**, 6271 (2008).

[16] A.E. Sikaily, A.E. Nemr, A. Khaled, O. Abdelwehab, *J. Hazard. Mater.* **148**, 216 (2007).

[17] World Health Organization (WHO), *Guidelines for drinking-water quality*, 3rd ed., Geneva 1:334, 2004.

[18] M.M. Amin, A. Khodabakhshi, M. Mozafari, B. Bina, S. Kheiri, *Environ. Eng. Manag. J.* **9**, 921 (2010).

[19] J. Hu, I.M.C. Lo, G. Chen, *Water Sci. Technol.* **50**, 139 (2004).

[20] R. Massart, *IEEE Trans. Magn.* **17**, 1247 (1981).

[21] W. Stöber, A. Fink, E. Bohn, *J. Coll. Interf. Sci.* **26**, 62 (1968).

[22] S. Brunauer, P.H. Emmett, E. Teller, *J. Am. Chem. Soc.* **60**, 309 (1938).

[23] APHA, *Standard Methods for the Examination of Water and Wastewater*, 19th ed., American Public Health Association, Washington, DC 1995.

[24] K. Nakamoto, *Infrared Spectra of Inorganic and Coordination Compounds*, 2nd ed., Wiley, London 1970.

[25] A. Evcin, N.Ç. Bezir, R. Kayalı, M. Kasıkçı, A. Oktay, *Acta Phys. Pol. A* **128**, B-303 (2015).

[26] S. Sadeghi, H. Azhdari, H. Arabi, A.Z. Moghaddam, *J. Hazard. Mater.* **215**, 208 (2012).

[27] X. Zhao, Y. Shi, T. Wang, Y. Cai, G. Jiang, *J. Chromatogr. A* **1188**, 140 (2008).

[28] S. Wang, J. Tang, H. Zhao, J. Wana, K. Chen, *J. Coll. Interf. Sci.* **432**, 43 (2014).

[29] J. Wang, S. Zheng, Y. Shao, J. Liu, Z. Xu, D. Zhu, *J. Coll. Interf. Sci.* **349**, 293 (2010).

[30] D. Mohan, C.U. Pittman, Jr., *J. Hazard. Mater. B* **137**, 762 (2006).

[31] H. Zhang, Y. Tang, D. Cai, X. Liu, X. Wang, Q. Huang, Z. Yu, *J. Hazard. Mater.* **181**, 801 (2010).

[32] U.K. Garg, M.P. Kaur, V.K. Garg, D. Sud, *Biores. Technol.* **99**, 1325 (2008).

[33] C. Namasivayam, D. Sangeetha, *J. Hazard. Mater.* **135**, 449 (2006).

[34] K. Fukushi, T. Sato, *Environ. Sci. Technol.* **39**, 1250 (2005).

[35] Y. Jung, J. Choi, W. Lee, *Chemosphere* **68**, 1968 (2007).

[36] P. Yuan, D. Liu, M. Fan, D. Yang, R. Zhu, F. Ge, J.X. Zhu, H. He, *J. Hazard. Mater.* **173**, 614 (2010).

[37] P. Yuan, M. Fan, D. Yang, H. He, D. Liu, A. Yuan, J. Zhu, T. Chen, *J. Hazard. Mater.* **166**, 821 (2009).

[38] W. Rieman, H. Walton, *Ion-Exchange in Analytical Chemistry*, International Series of Monographs in Analytical Chemistry, Vol. 38, Pergamon Press, Oxford 1970.